Am. J. Hum. Genet. 53:417–432, 1993

# Enzymological and Mutational Analysis of a Complex Primary Hyperoxaluria Type I Phenotype Involving Alanine:Glyoxylate Aminotransferase Peroxisome-to-Mitochondrion Mistargeting and Intraperoxisomal Aggregation

C. J. Danpure,* P. E. Purdue,* P. Fryer,† S. Griffiths,† J. Allsop,* M. J. Lumb,* K. M. Guttridge,† P. R. Jennings,* J. I. Scheinman,‡ S. M. Mauer,§ and N. O. Davidson||

*Biochemical Genetics Research Group and †Electron Microscopy Support Group, Medical Research Council Clinical Research Centre, Harrow, Middlesex; ‡Duke University Medical Center, Durham; §Variety Club Children's Hospital, University of Minnesota, Minneapolis; and ||Department of Medicine, University of Chicago, Chicago

## Summary

**Primary hyperoxaluria type 1 (PH1) is a rare autosomal recessive disease caused by a deficiency of the liver-specific peroxisomal enzyme alanine:glyoxylate aminotransferase (AGT). Three unrelated PH1 patients, who possess a novel complex phenotype, are described. At the enzymological level, this phenotype is characterized by a complete, or nearly complete, absence of AGT catalytic activity and reduced AGT immunoreactivity. Unlike normal individuals in whom the AGT is confined to the peroxisomal matrix, the immunoreactive AGT in these three patients was distributed approximately equally between the peroxisomes and mitochondria. The peroxisomal AGT appeared to be aggregated into amorphous core-like structures in which no other peroxisomal enzymes could be identified. Mutational analysis of the AGT gene showed that two of the three patients were compound heterozygotes for two previously unrecognized point mutations which caused Gly41→Arg and Phe152→Iso amino acid substitutions. The third patient was shown to be a compound heterozygote for the Gly41→Arg mutation and a previously recognized Gly170→Arg mutation. All three patients were homozygous for the Pro11→Leu polymorphism that had been found previously with a high allelic frequency in normal populations. It is suggested that the Phe152→Iso and Gly170→Arg substitutions, which are only eighteen residues apart and located in the same highly conserved internal region of 58 amino acids, might be involved in the inhibition of peroxisomal targeting and/or import of AGT and, in combination with the Pro11→Leu polymorphism, be responsible for its aberrant mitochondrial compartmentalization. On the other hand, the Gly41→Arg substitution, either in combination with the Pro11→Leu polymorphism or by itself, is predicted to be responsible for the intraperoxisomal aggregation of the AGT protein.**

## Introduction

Primary hyperoxaluria type 1 (PH1) is an autosomal recessive disease characterized biochemically by excessive synthesis of oxalate and glycolate and clinically by inappropriate deposition of calcium oxalate, as various combinations of urolithiasis, nephrocalcinosis, and systemic oxalosis (Williams and Smith 1983). The hyperoxaluria and hyperglycolic aciduria, characteristic of PH1, are caused by a failure to metabolize glyoxylate properly because of a deficiency of the liver-specific peroxisomal enzyme alanine:glyoxylate aminotransferase (AGT) (Danpure and Jennings 1986). Although the disease is extremely heterogeneous at the clinical level (Danpure 1991) and although tremendous advances in its treatment have been made recently (Watts et al. 1991), patients typically die of renal failure in early adulthood (Williams and Smith 1983).

PH1 is also heterogeneous at the enzymological level (Danpure and Jennings 1988; Danpure 1991). About

Received February 3, 1993; final revision received April 15, 1993.

Address for correspondence and reprints: Dr. C. J. Danpure, Biochemical Genetics Research Group, MRC Clinical Research Centre, Watford Road, Harrow, Middlesex HA1 3UJ, United Kingdom.



0002-9297/93/5302-0014$02.00

**Table 1**

**AGT Levels in the Livers of PH1 Patients and Their Families**

| | AGT | GGT | AGT* [a] | AGT% [b] | CRM [c] |
|---|---|---|---|---|---|
| Family 1: | | | | | |
| Patient 1 ..... | .38 | .85 | .00 | .0 | + |
| Mother 1a .... | 2.94 | .83 | 2.39 | 53.1 | +++ |
| Father 1b ..... | 4.00 | .96 | 3.36 | 74.7 | +++ |
| Family 2: | | | | | |
| Patient 2 ..... | .65 | | .25 [d] | 5.6 [d] | + |
| Mother 2a .... | 3.13 | .64 | 2.71 | 60.2 | +++ |
| Family 3: | | | | | |
| Patient 3 ..... | .48 | .83 | .00 | .0 | + |
| Others: | | | | | |
| Patient 4 ..... | .65 | .97 | .01 | .2 | + |
| Patient 5 ..... | .88 | 1.20 | .09 | 2.0 | +/− |
| Patient 6 ..... | .54 | .69 | .08 | 1.9 | +++++ |
| Normals: | | | | | |
| Mean ..... | 5.00 | .65 | 4.50 | 100.0 | +++++ |
| Range ..... | 3.25–8.99 | .38–.92 | 2.75–8.38 | 61.1–186.2 | |

NOTE.—Liver biopsies were not available for analysis for parents 2b, 3a, and 3b. Patient 6, although not referred to in the text of this paper, is used as a control for the PCRs and restriction analysis (see figs. 5–7).

[a] AGT* = AGT corrected for crossover from GGT (Danpure and Jennings 1988).

[b] AGT% = AGT* as a percentage of the mean normal value (normal values taken from Danpure and Jennings [1988]).

[c] CRM = subjective assessment of relative amount of AGT immunoreactive protein as determined by immunoblotting. +/− = Barely detectable; + and +++ = intermediate; and +++++ = normal.

[d] AGT* and AGT% values for patient 2 had to be estimated because there was not enough sample to measure GGT activity.

70% of patients have undetectable levels of AGT catalytic activity (ENZ−), while the remainder have activities that vary from 3%–48% of the mean normal activity (ENZ+). About two-thirds of the ENZ− patients also have no immunoreactive AGT protein (CRM−). In the remaining third of ENZ− patients and in all the ENZ+ patients, immunoreactive AGT protein is present (CRM+). This can vary from barely detectable levels to normal, or even supranormal, levels. In the ENZ+ patients, the level of immunoreactive AGT protein is usually approximately proportional to the level of enzyme activity.

In all the PH1 patients so far studied who are ENZ−/CRM+ (~20% of the total), the immunoreactive, but catalytically defunct, AGT protein is correctly localized totally within the peroxisomal matrix (Cooper et al. 1988*a*). However, in all the ENZ+/CRM+ patients so far studied, the intracellular distribution of AGT is very different. In these patients, who are predicted to constitute about one-third of the total, about 90% of the immunoreactive AGT protein is erroneously localized in the mitochondria (Danpure et al. 1989) with only about 10% correctly localized in the peroxisomes. AGT would appear not to be able to fulfill its proper metabolic function (i.e., glyoxylate transamination/detoxification) when located in mitochondria rather than in the peroxisomes.

The human AGT gene has been cloned and sequenced at both the cDNA (Takada et al. 1990) and genomic (Purdue et al. 1991*c*) levels and has been shown to exist as a single-copy gene located on chromosome 2q36-37. Various mutations in the AGT gene have been identified in PH1 patients, including those associated with the ENZ−/CRM− (Nishiyama et al. 1991; Minatogawa et al. 1992), ENZ−/CRM+ (Purdue et al. 1992*a*), and ENZ+/CRM+ (protein trafficking defect) (Purdue et al. 1990) phenotypes. In the last case, the characteristic enzymological phenotype is due to the cosegregation of a Pro11→Leu polymorphism (found in the normal Caucasian population, with an allelic frequency of about 15%) and a Gly170→Arg mutation. The Pro11→Leu substitution leads to the generation of an N-terminal amphiphilic α-helix which acts as a weak mitochondrial targeting sequence, whereas the Gly170→Arg substitution appears to directly interfere with the peroxisomal targeting/import of AGT (Purdue et al. 1990, 1991*a*). In this paper we report on the enzymological and mutational analysis of

a new complex phenotype, found in three apparently unrelated PH1 patients, characterized by partial peroxisome-to-mitochondrion mislocalization of AGT and the aggregation of peroxisomal AGT into core-like structures.

## Subjects, Material, and Methods

### *Patients*

Patient 1, a female, was 21 years old at the time of liver biopsy. She developed end-stage renal failure at the age of 16 years, at which time she exhibited nephrocalcinosis on abdominal X-ray examination. She was initially managed with hemodialysis and underwent living-related kidney transplantation which functioned adequately for approximately 2 years. Following nephrectomy, she was subsequently maintained on a combination of peritoneal dialysis and hemodialysis until the time of admission for combined kidney and liver transplantation.

Patient 2, a female, was 9 years old at the time of liver biopsy. She presented with end-stage renal failure secondary to nephrocalcinosis at the age of $3^1/_2$ mo and, after combined peritoneal and hemodialysis, received a living-related kidney transplantation at the age of 7 mo. The kidney functioned well for 2 years, but then failed after severe pneumococcal sepsis complicated by deposition of oxalate in the renal allograft. The patient then received a second living-related kidney transplantation which has functioned well for 7 years.

Patient 3 was 9 years old at the time of liver biopsy. She was a girl of normal growth who presented with poor urine control and microscopic hematuria. Renal ultrasound, and later pyelography, demonstrated bilateral medullary nephrolithiasis, with normal renal size and function. Oxalate excretion was markedly elevated (114–183 mg/24 h) and was unresponsive to pyridoxine. On therapy with thiazides, neutral phosphate, and high fluid intake, all parameters have remained stable for $1^1/_2$ years. In all patients, PH1 was confirmed by enzymic analysis of percutaneous needle liver biopsies (table 1).

### *Liver Biopsies and Enzyme Assays*

Percutaneous needle biopsies of the liver were taken, and portions were immediately frozen. After thawing, the samples were sonicated in 100 mM ice-cold phosphate buffer pH 7.4, containing 100 μM pyridoxal phosphate, to give a 10% (w/v) suspension (Danpure and Jennings 1988). Any nonsuspended fibrous material was removed by centrifugation at 500 *g* for 10 min. The supernatants were used for the enzyme and protein assays.

AGT was measured either by a macro spectrophotometric method (Danpure and Jennings 1988) or a micro radiochemical method (Allsop et al. 1987), depending on the size of the biopsy. When enough material was available, glutamate:glyoxylate aminotransferase (GGT) was also measured by a spectrophotometric method, as described elsewhere (Danpure and Jennings 1988). Protein was measured by the method of Lowry et al. (1951), using BSA as standard.

### *Antibodies*

AGT was purified from human liver to a single silver-staining band on SDS-PAGE, similar to the procedure described by Thompson and Richardson (1967). The purified protein was used to raise antibodies in New Zealand white rabbits by conventional methods. These antibodies recognized a single band in fresh normal human liver, after SDS-PAGE and immunoblotting. In some cases the antisera were absorbed against a CRM− human liver homogenate, and from this IgG was prepared by sodium sulphate fractionation. Antiserum against catalase was prepared similarly by using commercial human erythrocyte catalase (Calbiochem) as the antigen. The rabbit antibodies against rat peroxisomal thiolase, peroxisomal hydratase, and acyl-CoA oxidase were a gift from Professor A. Völkl (University of Heidelberg), the rabbit anti-rat glycolate oxidase from Professor T. Hashimoto (Shinshu University School of Medicine), and the rabbit anti-rat urate oxidase antibody from Dr. S. Yokota (Yamanashi Medical College).

### *Immunoblotting*

Samples of liver sonicates containing 50 μg protein were electrophoresed on SDS-PAGE, as described by Laemmli (1970) and electroblotted onto nitrocellulose membranes by the procedure described by Towbin et al. (1979). The membranes were incubated with rabbit anti-human AGT IgG (diluted 1 in 200 with 100 mM PBS pH 7.2, containing 3% milk proteins) for 4 h at room temperature (Wise et al. 1987). After washing with PBS, the bound antibodies were visualized using alkaline phosphatase conjugated to goat anti-rabbit IgG and developed using the p-toluidine salt of 5-bromo-4-chloro-3-indolyl phosphate and p-nitroblue tetrazolium chloride (Bio-Rad). Purified human liver AGT (50–200 ng) and Rainbow Molecular Weight Markers (Amersham International) were run alongside the liver samples.

### *Immunoelectron Microscopy*

Immediately after biopsy, portions of each liver sample were fixed in 1% glutaraldehyde in 100 mM phos-

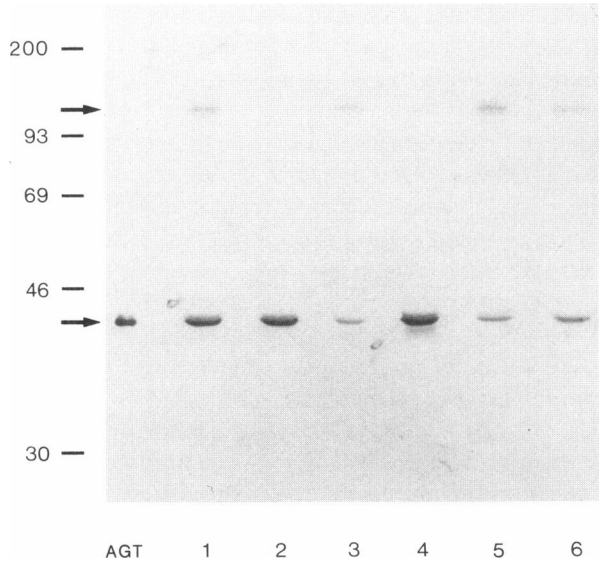


**Figure 1** AGT immunoblotting of liver samples from PH1 patients and their parents. Liver sonicates (containing 50 μg protein) were run on SDS-PAGE and immunoblotted with rabbit anti-human AGT IgG (see Material and Methods). Lane AGT, Purified AGT standard (100 ng). Lane 1, Parent 1a. Lane 2, Parent 1b. Lane 3, Patient 1. Lane 4, Parent 2a. Lane 5, Patient 2. Lane 6, Patient 3. Numbers on left of blot indicate molecular masses of standards (Rainbow Molecular Weight Markers; Amersham International). Arrows indicate normal size immunoreactive AGT protein (~43 kDa) and abnormal high-molecular-mass band of 110–120 kDa (lanes 1, 3, 5, and 6 only).

phate buffer pH 7.2 for 1–2 h at room temperature. They were then transferred to the buffer and stored at 4°C (Cooper et al. 1988*a*). After blocking the free aldehyde groups with 500 mM ammonium chloride for 30 min at room temperature, the samples were washed in buffer, dehydrated, and embedded by a modification of the method described elsewhere (Cooper et al. 1988*a*; Danpure et al. 1990). Dehydration was carried out with a graded methanol series from 0%–90% at progressively lower temperatures, down to −20°C. Infiltration with Lowicryl K4M (Carlemalm et al. 1982) was carried out at this temperature by using the following procedure: 90% methanol:Lowicryl (1:1) for 1 h, 90% methanol:Lowicryl (1:3) for 1 h, neat Lowicryl overnight, replacement with fresh Lowicryl, and then polymerization at −25°C by UV irradiation overnight. Further polymerization was carried out at room temperature after inverting the capsules containing the tissue. Ultrathin sections (nominally 60 nm) were mounted on formvar/carbon-coated copper grids.

Immunolabeling was carried out by a procedure modified from that of Roth (1982) (see Danpure et al. 1990). All steps were carried out at room temperature on 20-μl droplets on Parafilm for 1 h. Washes were for 5 min. For single labeling, we used the following method: step 1, PBS plus 3% BSA; step 2, protein A (100 μg/ml) in PBS/BSA; step 3, three washes in PBS/BSA; step 4, rabbit anti-human AGT antiserum diluted 1:500 or anti-catalase diluted 1:100 in PBS/BSA; step 5, three washes in PBS/BSA; step 6, protein A-gold (20 nm; Biocell, Cardiff, U.K.) diluted 1:100 in PBS/BSA; and step 7, two washes in PBS, stream wash in distilled water. For double labeling, we used the same method as that for single labeling up to and including step 5; then we used the following method: step 6, protein A-gold (10 nm) diluted 1:100 in PBS/BSA; step 7, three washes in PBS/BSA; step 8, protein A (100 μg/ml); step 9, three washes in PBS/BSA; step 10, second antibody; step 11, three washes in PBS/BSA; step 12, protein A-gold (20 nm); step 13, two washes in PBS; and step 14, stream wash in distilled water. After immunolabeling, the grids were stained in aqueous uranyl acetate for 20 min, followed by lead citrate for 1 min.

### *RNA/DNA Preparation*

Genomic DNA was prepared from whole blood by using standard procedures (Sambrook et al. 1989). Total hepatic RNA was prepared from the liver of patient 1, after total hepatectomy, by using a modification (Teng et al. 1990) of the method of Chomczynski and Sacchi (1987). First-strand cDNA was prepared by reverse transcription of total RNA from patient 1, as described elsewhere (Purdue et al. 1990), except that oligo(dT) was used as the primer.

### *PCR, Cloning, Sequencing, and Restriction Analysis*

cDNA and exon-specific genomic PCR, cloning, dideoxy-sequencing, and restriction enzyme analysis were carried out using standard protocols (Sambrook et al. 1989), delineated more precisely where relevant in the text. The following PCR oligonucleotide primers were used: P1, 5′-GCACAGATAAGCTTCAGGGA-3′ (−39 to −20, exon 1); P2, 5′-CTTGAAGGATGGATCCAGGG-3′ (+47 to +28, exon 2); P3, 5′-CCCTCTGAGCTCCACCCACA-3′ (−38 to −19, exon 4); P4, 5′-TCTGAGCTGAGCTCCAGTCC-3′ (+42 to +23, exon 4); P5, 5′-CTGCAGCCCCTTGATGGCTCC-3′ (cDNA 609–629); P6, 5′-CACCAATCCTCACCTCTCAC-3′ (cDNA 14–33); and P7, 5′-GAGACTTGCAGGGTCTGTTT-3′ (cDNA 1389–1370). P1, P3, P5, and P6 are top-strand primers. P2, P4, and P7 are reverse-strand primers. The nucleotides are numbered relative to the 5′ end of the cDNA sequence (Takada et al. 1990). P1 maps to a nontranscribed region 39–20 bases upstream

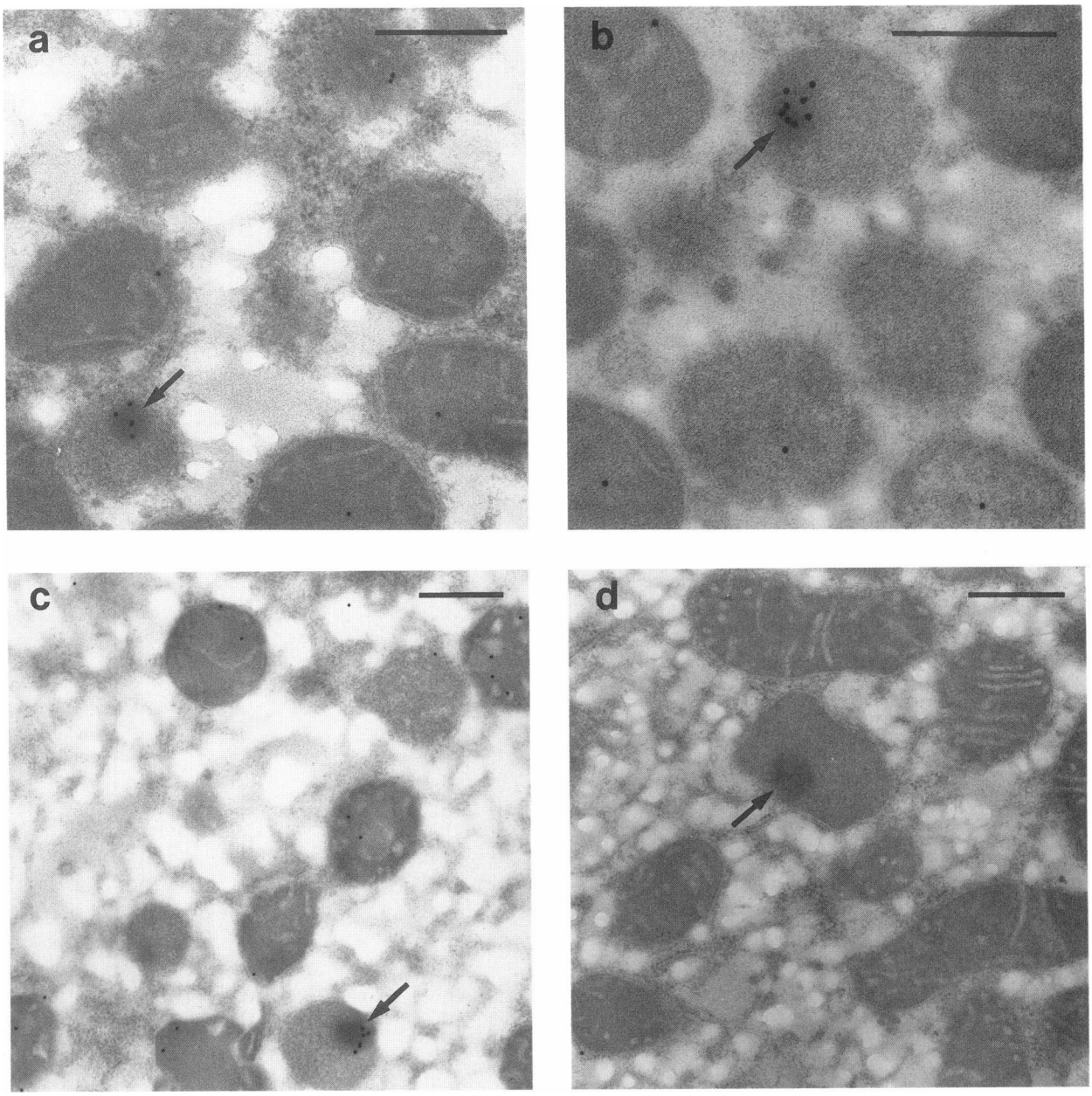


**Figure 2** Intracellular compartmentalization of AGT in the livers of three PH1 patients. Liver sections from patient 2 (*a*), patient 1 (*b*), and patient 3 (*c*) were labeled for AGT by postembedding protein A-gold immunocytochemistry (see Material and Methods) and were compared with a section from patient 2, incubated with preimmune rabbit serum (*d*). Arrows indicate the intraperoxisomal cores; bars represent 0.5 μm. Note the concentration of 20-nm gold particles over the peroxisomal cores and the low, but significant, level of mitochondrial immunolabeling.

of the start of exon 1. P2–P4 map to intronic sequences as follows: P2 to 28–47 bases downstream of exon 2, P3 to 38–19 bases upstream of exon 4, and P4 to 23–42 bases downstream of exon 4. P5–P7 map to cDNA sequences as follows: P5 to cDNA nucleotides 609–629 (maps in exon 4), P6 to cDNA nucleotides 14–33 (in the 5′ UTR [untranslated region]), and P7 to cDNA nucleotides 1389–1370 (in the 3′ UTR). Primer pairs P1/P2 and P3/P4 were used for the PCR amplification from genomic DNA of exons 1+2 and 4, respectively. PCR with primers P5/P4 was used to detect the previously known G630→A mutation in exon 4 (see table 3), without having to resort to allele-specific oligonucleotide hybridization (Purdue et al. 1990). A single-base

**Table 2**

**Quantitation of Immunoelectron Microscopic Observations**

| | Morphological Characteristics | | | Labeling Characteristics | | | |
|---|---|---|---|---|---|---|---|
| | | Mean Diameters (SD) (nm) | | Gold Particles per Organelle (×10) | | | |
| | % Peroxisomes with Cores | Peroxisomes | Cores | Peroxisomes | Mitochondria | % Peroxisome Label on Cores | % Mitochondrial Labeling[a] |
| Family 1: | | | | | | | |
| Patient 1 ..... | 21 | 349 (104) | 129 (29) | 38 | 7 | 99 | 52.5 |
| Mother 1a ..... | 6 | 366 (97) | 138 (19) | 150 | 2 | 7 | 7.4 |
| Father 1b ..... | <1 | 385 (136) | ... | 76 | 7 | ... | 35.6 |
| Family 2: | | | | | | | |
| Patient 2 ..... | 31 | 329 (111) | 129 (32) | 43 | 10 | 88 | 58.3 |
| Mother 2a ..... | 1 | 419 (117) | ... | 154 | 4 | ... | 13.5 |
| Family 3: | | | | | | | |
| Patient 3 ..... | 34 | 404 (124) | 167 (33) | 33 | 14 | 89 | 71.8 |
| Normal control[b] ... | <1 | 425 (125) | ... | 335 | <.5 | ... | <1.0 |

NOTE.—For the determination of the morphological characteristics of the peroxisomes, 201–376 peroxisomes were measured. Too few cores were identified in parents 1b and 2a and the normal control to carry out any meaningful measurements. Full-scale morphometric analysis of labeling characteristics was not undertaken. Instead, gold labeling was determined on 12–40 peroxisomes and 33–137 mitochondria for each individual, and the overall value is quoted. Labeling was never found on the rare cores in parents 1b and 2a or the normal control.

[a] % mitochondrial labeling is estimated from the mean number of gold particles per organelle, assuming that the overall mitochondrial profile area is ~6 times greater per cell than the overall peroxisomal profile area (i.e., the mitochondrial compartment is 6 times bigger than the peroxisomal compartment) (see Danpure et al. 1989).

[b] Homozygous for the major AGT allele. A previous study (Purdue et al. 1990) showed that an individual homozygous for the minor AGT allele (i.e., that encoding the Pro11→Leu polymorphism) had ~5% AGT located in the mitochondria.

mismatch (underlined) in P5 forces the introduction of an *Msp*I restriction site after PCR, which is lost in the presence of the mutation. Primers P6/P7 were used for the PCR amplification of the complete coding region of the cDNA from patient 1.

## Results

### *AGT Catalytic Activity*

The AGT catalytic activities in the liver samples from all three patients (1, 2, and 3) were markedly deficient (table 1). When corrected for crossover from GGT (Danpure and Jennings 1988), the activities in two of the patients (1 and 3) were zero. Because of the very small size of the biopsy from the remaining patient (2), a GGT correction could not be made with confidence but could instead only be estimated. This patient had an apparent AGT activity of 5.6% of the mean normal value. The parents of patient 1 (1a and 1b) and the mother of patient 2 (2a) had corrected AGT activities varying between 53% and 75% of the mean normal value (table 1). These data unambiguously confirm the diagnosis of PH1 in these patients. The AGT values found in the parents are compatible with what would be expected in obligate heterozygotes.

### *AGT Immunoreactivity*

Immunoblotting analysis, following SDS-PAGE, showed that there was a marked reduction of 43-kDa immunoreactive AGT protein in patients 1, 2, and 3, and mildly reduced levels in the parents 1a, 1b, and 2a (fig. 1 and table 1). In addition to the normal 43-kDa immunoreactive band, patients 1, 2, and 3 and parent 1a also possessed a faint band of higher molecular mass (~110–120 kDa). This band has not been found previously in normal controls or other PH1 patients and was not found in parents 1b or 2a in the present study (fig. 1).

### *Immunoelectron Microscopy*

Examination of the intracellular localization of immunoreactive AGT protein by postembedding protein A-gold immunoelectron microscopy showed that the AGT had a bicompartmental distribution in all three patients (fig. 2). Compared to normal control individuals, the patients had reduced levels of immunoreactive AGT which, rather than being entirely peroxisomal, was distributed approximately equally between the peroxisomes and mitochondria (fig. 2 and table 2). Unusually, many (21%–34%) of the peroxisomal profiles con-

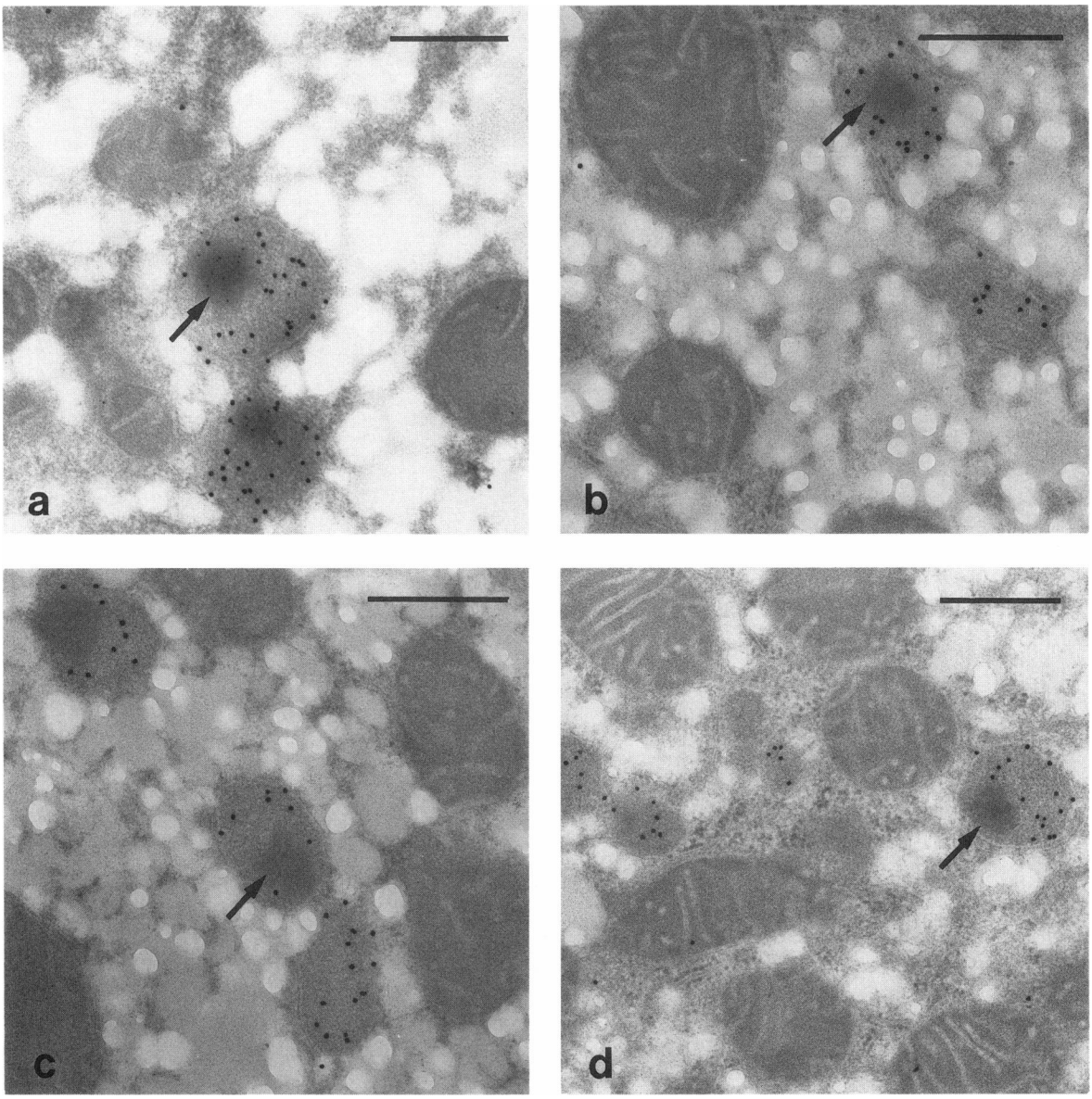


**Figure 3** Intracellular compartmentalization of various peroxisomal enzymes in the livers of PH1 patients. Liver sections from patient 3 (*a*) or patient 2 (*b–d*) were either double labeled for AGT (10 nm gold) and catalase (20 nm gold) (*a*) or single labeled (20 nm gold) for acyl-CoA oxidase (*b*), peroxisomal thiolase (*c*), and peroxisomal hydratase (*d*). Arrows indicate peroxisomal cores; bars represent 0.5 μm. Note the concentration of 10-nm gold particles (AGT) over the cores (*a*) but the avoidance of these cores by the 20-nm gold particles—catalase (*a*), acyl-CoA oxidase (*b*), peroxisomal thiolase (*c*), and peroxisomal hydratase (*d*).

tained dense amorphous core-like structures, and, when present, it was these structures rather than the peroxisomal matrix that were immunoreactive for AGT. In fact, 88%–99% of the total peroxisomal AGT immunoreactivity was located on the cores (table 2), whereas there was generally no immunoreactive AGT in peroxisomal profiles without cores. When antibodies to other peroxisomal enzymes were used (e.g., catalase, glycolate oxidase, acyl-CoA oxidase, peroxisomal thiolase, and hydratase), the immunoreactivity was confined to the peroxisomal matrix, and the cores were unreactive (fig. 3). With these latter antibodies, the level of peroxisomal immunoreactivity was independent of the presence or absence of cores. Neither the peroxisomal matrix nor cores were immunoreactive for urate oxidase (data not shown). When present, the mean di-

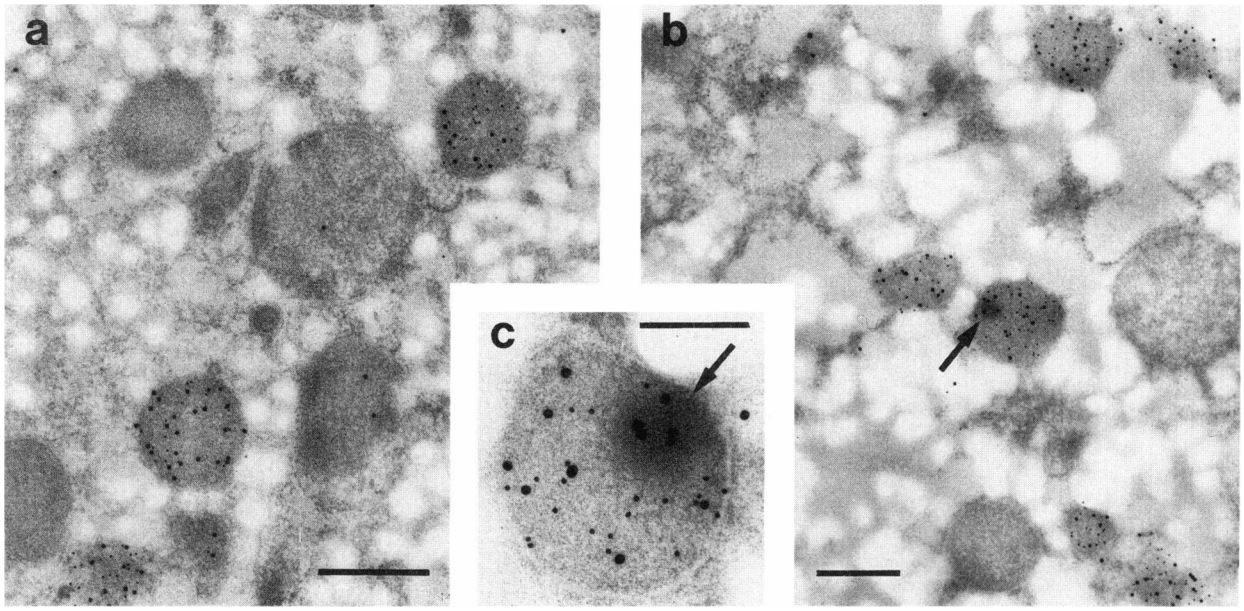


**Figure 4** Intracellular compartmentalization of AGT and catalase in the livers of two PH1 parents. Liver sections from parent 1b (*a*) and parent 1a (*b* and *c*) were double labeled for catalase (10 nm gold) and AGT (20 nm gold). Arrows indicate peroxisomal cores; bars represent 0.5 μm (*a* and *b*) or 0.25 μm (*c*). Note in parent 1b (*a*) the absence of peroxisomal cores and the presence of a low level of mitochondrial immunolabeling and in parent 1a (*b* and *c*) the presence of peroxisomal cores which label for AGT but not for catalase, while the peroxisomal matrix labels for both AGT and catalase. In parent 1a mitochondrial AGT immunolabeling was low and not detectable in this micrograph (*b*).

ameter of the peroxisomal cores was about 37%–41% of the mean peroxisomal profile diameter (table 2).

The peroxisomal AGT immunoreactivity in the parents 1a, 1b, and 2a was somewhat lower than normal, as expected for obligate heterozygotes (fig. 4 and table 2). Parents 1a, 1b, and 2a also showed variable amounts of mitochondrial AGT immunoreactivity, most apparent in parent 1b (estimated to be about 36% of the total label). Parent 1a also had a small number (about 6%) of peroxisomes containing core-like structures which, in addition to the matrix, were immunoreactive for AGT (table 2 and fig. 4). The peroxisomal cores in this parent were not immunoreactive for catalase, which was confined to the peroxisomal matrix. Because of the higher matrix AGT immunoreactivity in parent 1a, compared with that in her daughter (patient 1), only about 7% of the peroxisomal label was present on the cores. Core-like structures were found very rarely in the other parents and controls and, when present, were not immunoreactive for AGT.

### *Mutational Analysis*

Total RNA was prepared from the liver of patient 1, and northern blotting demonstrated the presence of AGT mRNA of apparently normal size and abundance (data not shown). Following reverse transcription PCR, using primers P6 and P7, a *Ssp*I-*Pvu*II cDNA fragment, containing the whole coding region, was cloned from this patient and sequenced. Four types of clone were identified, containing various combinations of two novel point mutations, G243→A and T576→A (see table 3). Most clones contained one or the other of these mutations. However, occasional clones contained both or neither. Such apparent phase disruptions have been noticed by others after the PCR amplification and cloning of heterozygous sequences (Jansen and Ledley 1990) and attributed to various combinations of PCR mispriming and bacterial recombination/mismatch repair. No other differences from the normal published sequence for AGT cDNA (Takada et al. 1990) were found, except that all clones contained the C154→T and A1142→G polymorphisms of the minor AGT allele (see table 3) reported elsewhere (Purdue et al. 1990).

The G243→A mutation causes the loss of an *Msp*I restriction site (fig. 5*a*); the T576→A mutation causes the gain of an *Mbo*I site (fig. 6*a*); and the C154→T polymorphism causes the loss of a *Sty*I site (see Purdue et al. 1990). Restriction digestion of total P6/P7 cDNA PCR product from patient 1 confirmed the heterozygosity of both mutations and the homozygosity of the polymorphism (data not shown). G243→A and

**Table 3**

**Mutations and Polymorphism Described in the Text and Their Predicted Effects on the AGT Amino Acid Sequence**

| | Nucleotide Substitution[a] | Exon Location | Amino Acid Replacement[a] |
|---|---|---|---|
| Polymorphism[b] .... | C154→T | 1 | Pro11→Leu |
| Mutations ..... | G243→A | 1 | Gly41→Arg |
| | T576→A | 4 | Phe152→Iso |
| | G630→A | 4 | Gly170→Arg |

[a] Nucleotide and amino acid substitutions refer to point replacements at the cDNA and protein sequence positions specified (see Takada et al. 1990).

[b] The polymorphism is that encoded by the less common (minor) AGT allele. In addition to the C154→T nucleotide substitution, which leads to a Pro11→Leu amino acid replacement, the minor allele also possesses an A1142→G substitution, which leads to an Iso340→Met replacement (Purdue et al. 1990) and a 74-bp intron 1 duplication (Purdue et al. 1991*b*). So far, functional significance has been attributed only to the Pro11→Leu replacement. The frequency of the minor allele in Caucasian populations has been variously estimated to be 5%–15% (Purdue et al. 1990, and unpublished observations).

C154→T map to exon 1 and T576→A maps to exon 4 of the AGT gene (see Purdue et al. 1991*c*). Exon-specific PCR and restriction digestion analysis of genomic DNA from patient 1 and her parents (1a and 1b) clearly demonstrated the compound heterozygosity of this patient, each parent carrying only one of the mutations (parent 1a carrying G243→A, and parent 1b carrying T576→A) (figs. 5*b* and 6*b*, respectively). Similarly, it was shown that patient 1 and both her parents (1a and 1b) were homozygous for the C154→T polymorphism (data not shown).

Material was not available for RNA preparation from patients 2 and 3. However, exon-specific PCR/restriction digestion analysis of genomic DNA from patient 2 demonstrated the presence of the same two mutations as found in patient 1 heterozygously. Studies on the parents 2a and 2b showed that patient 2, like patient 1, was a compound heterozygote, the two mutations being present on different alleles (data not shown). In addition, patient 2 and her mother (2a) were homozygous for the C154→T polymorphism, whereas the father (2b) was heterozygous. Similar studies on patient 3 and her parents (3a and 3b) demonstrated a somewhat different picture. In the case of this patient, although G243→A was present heterozygously (fig. 5*c*), T576→A was absent (data not shown). An exon-specific genomic PCR/restriction digestion screen of patient 3 showed the presence of a G630→A mutation heterozygously (fig. 7*b*), which had been found before in PH1 patients with the peroxisome-to-mitochondrion AGT targeting defect (Purdue et al. 1990). Again, studies on the parents, which showed that parent 3a carried G630→A (fig. 7*b*) and that parent 3b carried G243→A (fig. 5*c*), indicated that these two mutations were present on different alleles in patient 3. In addition, patient 3 and her mother (3a) were homozygous for the C154→T polymorphism, and her father (3b) was heterozygous. Analysis of all three patients and their parents demonstrated that all three mutations (i.e., G243→A, T576→A, and G630→A) always cosegregated with the minor (i.e., less common) AGT allele (i.e., that possessing the C154→T polymorphism) (Purdue et al. 1990).

### *Mutation/IEM Screening of Other PH1 Patients and Controls*

Exon-specific PCR/restriction digestion screening of numerous normal controls failed to reveal the presence of any of the three mutations. However, when a population of previously studied PH1 patients was screened, although G243→A was not found, T576→A was found in two individuals (patients 4 and 5). Previous studies had already shown that G630→A was present in about one-third of PH1 patients, in most cases heterozygously but occasionally homozygously (Purdue et al. 1990).

Enzymological, immunoblotting, and immunoelectron microscopic analysis of patients 4 and 5 showed them both to be markedly deficient in AGT catalytic activity and immunoreactive AGT protein (see table 1). Peroxisomal cores could not be found, and the low residual levels of immunoreactive AGT appeared to be localized mainly in the mitochondria (data not shown). Neither patient 4 nor 5 possessed G630→A, which is usually associated with the presence of mitochondrial AGT. Patient 4 was homozygous, and patient 5 heterozygous, for the minor allele, confirming the segregation of T576→A with the C154→T polymorphism.

## Discussion

The PH1 patients 1, 2, and 3 appear to possess a novel complex enzymological phenotype which can be divided into two parts, (1) aggregation of AGT within the peroxisomes into amorphous core-like structures and (2) partial intracellular mislocalization of AGT from the peroxisomes to the mitochondria. These characteristics are superimposed upon a generalized marked deficiency of AGT catalytic activity and reduction in the levels of AGT immunoreactive protein.

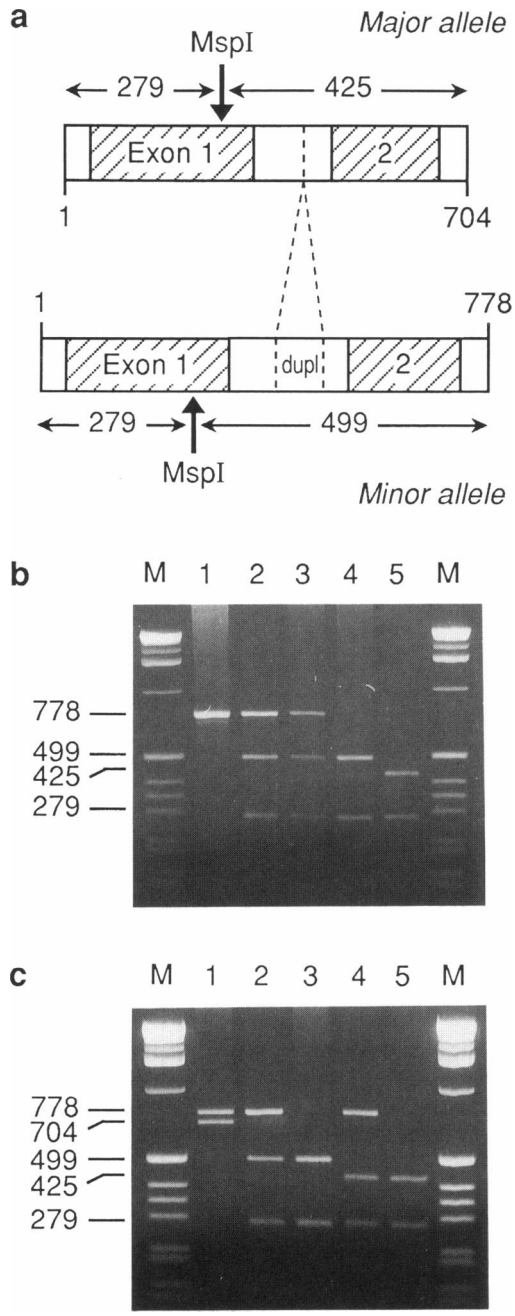


**Figure 5** Exon-specific genomic PCR/*Msp*I restriction analysis of the G243→A mutation in various PH1 patients and their parents. *a*, Genomic DNA amplified by PCR using primers P1 and P2. This produces a 704-bp fragment from the more common major allele but a 778-bp fragment from the less common minor allele, because of the presence of a 74-bp duplication (dupl) in intron 1 (see Purdue et al. 1991*b*). The G243→A mutation, which has only ever been found on the background of the minor allele (i.e., that possessing the C154→T polymorphism), leads to the loss of an *Msp*I site (↑). After *Msp*I digestion, the major allele always produces two bands of 425 bp and 279 bp, whereas the minor allele produces two bands of 499 bp and 279 bp, if the mutation is absent, or one band of 778 bp, if the mutation is present. Hatched areas represent exons 1 and 2; unblackened areas represent part of the upstream untranscribed region, all of intron 1, and part of intron 2. *b*, Agarose gel (2%) of PCR/*Msp*I digestion products from family 1. Lane 1, Undigested PCR product from parent 1b. Lanes 2–5, *Msp*I-digestion products from patient 1 (lane 2), parent 1a (lane 3), parent 1b (lane 4), and patient 6 as a control (lane 5). Lane M, Molecular weight markers. These results are compatible with the following genotypes: patient 1 = T154/T154, G243/A243; parent 1a = T154/T154, G243/A243; parent 1b = T154/T154, G243/G243; and patient 6 (control) = C154/C154, G243/G243. *c*, Agarose gel (2%) of PCR/*Msp*I digestion products from family 3. Lane 1, Undigested PCR product from parent 3b. Lanes 2–5, *Msp*I digestion products from patient 3 (lane 2), parent 3a (lane 3), parent 3b (lane 4), and patient 6 as a control (lane 5). Lane M, Molecular weight markers. These results are compatible with the following genotypes: patient 3 = T154/T154, G243/A243; parent 3a = T154/T154, G243/G243; parent 3b = C154/T154, G243/A243; and patient 6 (control) as for (*b*). The genotypes deduced for family 2 (data not shown) were the same as those found for family 3, i.e., patient 2 = T154/T154, G243/A243; parent 2a = T154/T154, G243/G243; and parent 2b = C154/T154, G243/A243. Note that the C154→T polymorphism of the minor allele cosegregates absolutely with the intron 1 duplication. However, in all patients and parents, the presence/absence of this polymorphism, which leads to the loss of a *Sty*I site, was confirmed separately by *Sty*I restriction digestion (data not shown).

Although intraperoxisomal cores are frequently found in the tissues of some mammals, they are rarely found in human liver. In species in which cores are normally found, they consist largely of crystalline urate oxidase (Angermuller and Fahimi 1986; Völkl et al. 1988). During the evolution of hominids, however, expression of this enzyme has been lost (Afzelius 1965; Varela Echavarria et al. 1988). The human urate oxidase gene, despite being otherwise well conserved, is nonfunctional because of the presence of various nonsense mutations (Wu et al. 1989; Yeldandi et al. 1990). Core-like structures are sometimes, but rarely, found in human peroxisomes (Biempica 1966; Sternlieb and Quintana 1977; Grzybek et al. 1986; Collins et al. 1989), but in most cases these have not been characterized. However, in a study by De Netto et al. (1991), two of nine patients with colorectal cancer appeared to possess peroxisomal cores, apparently with urate oxidase catalytic activity. In the present study, no evidence was found for a "reactivation" of the urate oxidase gene. No increase in urate oxidase catalytic activity could be detected in patient 1, and immunoreactive urate oxidase could not be detected in the peroxisomal cores (or matrix) of any of the patients.

The composition of the peroxisomal cores found in the present study cannot be known with any certainty. However, the fact that they label with antibodies to AGT but not with antibodies to six other peroxisomal

enzymes opens up the possibility that the cores are actually composed of AGT. Such apparent intraorganellar aggregation of an otherwise soluble peroxisomal protein has not been found before. Alternatively, the mutant AGT might have bound to some otherwise invisible peroxisomal matrix protein with which other peroxisomal enzymes do not interact. In this respect, it is interesting to note that the presence of a higher molecular mass band of 110–120 kDa, detected by anti-AGT antibody on SDS-PAGE, appeared to be correlated with the presence of peroxisomal cores, not only

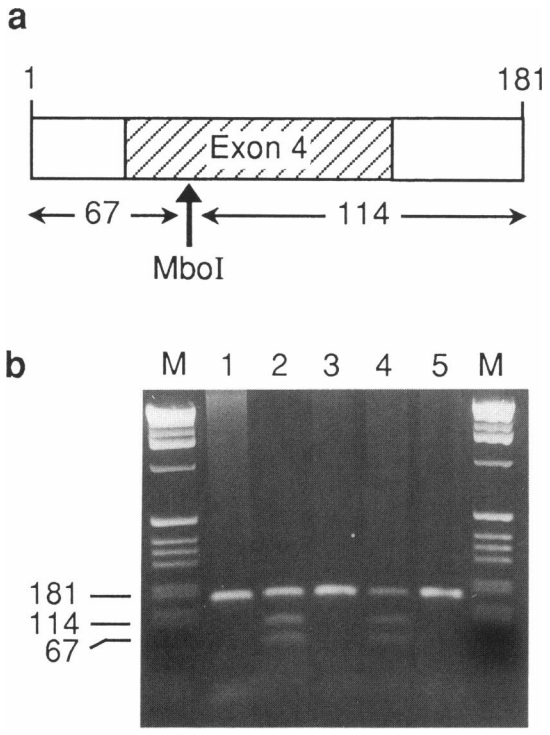


**Figure 6** Exon-specific genomic PCR/*Mbo*I restriction analysis of the T576→A mutation in various PH1 patients and their parents. *a*, Genomic DNA amplified by PCR using primers P3 and P4, producing a fragment of 181 bp. The T576→A mutation leads to the gain of an *Mbo*I site (↑) which cuts the PCR product into two fragments of 114 bp and 67 bp. Hatched area represents exon 4; and unblackened areas represent introns. *b*, Agarose gel (2%) of PCR/*Mbo*I digestion products from family 1. Lane 1, Undigested PCR product from parent 1b. Lanes 2–5, *Mbo*I digestion products from patient 1 (lane 2), parent 1a (lane 3), parent 1b (lane 4), and patient 6 as a control (lane 5). Lane M, Molecular weight markers. These results are compatible with the following genotypes: patient 1 = T576/A576; parent 1a = T576/T576; parent 1b = T576/A576; and patient 6 (control) = T576/T576. The genotypes deduced for family 2 (data not shown) were as follows: patient 2 = T576/A576; parent 2a = T576/A576; parent 2b = T576/T576; and patient 6 (control) as for (*b*). The genotypes deduced for family 3 (data not shown) were all normal, i.e., T576/T576.

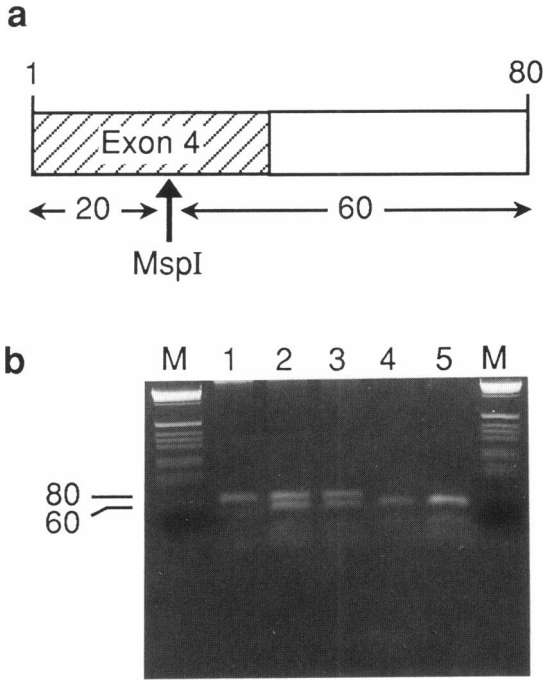


**Figure 7** Exon-specific genomic PCR/*Msp*I restriction analysis of the G630→A mutation in various PH1 patients and their parents. *a*, Genomic DNA was amplified by PCR using primers P5 and P4, producing a fragment of 80 bp. The G630→A mutation does not produce an RFLP. Therefore a T→C mismatch was introduced into primer P5 at the penultimate 3′ nucleotide position in order to introduce an *Msp*I site (↑) after PCR amplification (see Material and Methods). *Msp*I cuts the P5/P4 PCR product in two fragments of 60 bp and 20 bp. The presence of the mutation leads to the loss of this *Msp*I site. Hatched area represents part of exon 4; and unblackened area represents the intron. *b*, Agarose gel (3%) of PCR/*Msp*I digestion products from family 3. Lane 1, Undigested PCR product from parent 3b. Lanes 2–5, *Msp*I digestion products from patient 3 (lane 2), parent 3a (lane 3), parent 3b (lane 4), and patient 6 as a control (lane 5). Lane M, Molecular weight markers. These results are compatible with the following genotypes: patient 3 = G630/A630; parent 3a = G630/A630; parent 3b = G630/G630; and patient 6 (control) = G630/G630. The genotypes deduced for families 1 and 2 (data not shown) were all normal, i.e., G630/G630.

in patients 1, 2, and 3, but also in parent 1a. This band was refractory to extensive boiling with 10% SDS and 5% mercaptoethanol, indicating its covalent, nondisulfide nature. The molecular identity of this band has yet to be determined, but it might be a complex of AGT bound to one or more other proteins. Whether this is functionally or mechanistically related to the intraperoxisomal aggregation phenomenon is not known.

Although many mammals possess significant quantities of AGT within the mitochondria (for example, see Danpure et al. 1990), most normal humans localize AGT exclusively to the peroxisomes (Noguchi and Ta-

## Table 4

**Summary of Amino Acid Substitutions Found in Patients and Their Parents, Compared with Their Enzymological Phenotypes**

| | Amino Acid Substitutions at Residue No.[a] | | | | Enzymological Phenotypes | |
|---|---|---|---|---|---|---|
| | 11 | 41 | 152 | 170 | Mitochondrial AGT | Peroxisome Cores[b] |
| Normals: | | | | | | |
| Major allele ..... | Pro | Gly | Phe | Gly | − | − |
| Minor allele ..... | (Leu) | · | · | · | +/− | − |
| Family 1: | | | | | | |
| Patient 1 ..... | (Leu)<br>(Leu) | Arg<br>· | ·<br>Iso | ·<br>· | + | + |
| Mother 1a ..... | (Leu)<br>(Leu) | Arg<br>· | ·<br>· | ·<br>· | +/− | +/− |
| Father 1b ..... | (Leu)<br>(Leu) | ·<br>· | Iso<br>· | ·<br>· | + | − |
| Family 2: | | | | | | |
| Patient 2 ..... | (Leu)<br>(Leu) | Arg<br>· | ·<br>Iso | ·<br>· | + | + |
| Mother 2a ..... | (Leu)<br>(Leu) | ·<br>· | Iso<br>· | ·<br>· | + | − |
| Father 2b ..... | (Leu)<br>· | Arg<br>· | ·<br>· | ·<br>· | ? | ? |
| Family 3: | | | | | | |
| Patient 3 ..... | (Leu)<br>(Leu) | Arg<br>· | ·<br>· | ·<br>Arg | + | + |
| Mother 3a ..... | (Leu)<br>(Leu) | ·<br>· | ·<br>· | Arg<br>· | ? | ? |
| Father 3b ..... | (Leu)<br>· | Arg<br>· | ·<br>· | ·<br>· | ? | ? |
| Others[c]: | | | | | | |
| Patient 4 ..... | (Leu)<br>(Leu) | ·<br>· | Iso<br>· | ·<br>· | + | − |
| Patient 5 ..... | (Leu)<br>· | ·<br>· | Iso<br>· | ·<br>· | + | − |
| Patient 6 ..... | ·<br>· | ·<br>· | ·<br>· | ·<br>· | − | − |

NOTE.—The allelic segregation of mutations (amino acid substitutions) and the Pro11→Leu polymorphism, either determined directly or deduced from the family studies, are represented by individual lines.

[a] (Leu) = polymorphic variation encoded by the minor AGT allele; "·" = identity with the peptide sequence encoded by the major AGT allele.

[b] Peroxisome cores = presence of AGT immunoreactive peroxisomal cores; for the normals these phenotypes are for those individuals homozygous for either the major or minor AGT alleles.

[c] In patients 4 and 5, the apparently "normal" allele is probably not expressed. In all other individuals, both alleles are expressed. Patient 6, who is homozygous for the major AGT allele and does not possess any of the mutations described in this paper, is used as a control for the mutational analysis.

kada 1978, 1979; Yokota et al. 1987; Cooper et al. 1988*a*, 1988*b*). The exception to this is individuals possessing the less common minor AGT allele (i.e., that possessing the Pro11→Leu polymorphism, see table 3), homozygotes of which target about 5% of their AGT to the mitochondria, with the remaining 95% imported into the peroxisomes. However, in a large proportion (estimated to be about 30%) of PH1 patients, most (~90%) of the the AGT is localized within the mitochondria (Danpure et al. 1989). Mitochondrial AGT is


**Figure 8** Amino acid sequence of AGT. The amino acid sequence of AGT, as deduced from the published cDNA sequence (Takada et al. 1990), is shown together with the locations of the amino acid substitutions (Gly41→Arg, Phe152→Iso, and Gly170→Arg) caused by the mutations (G243→A, T576→A, and G630→A, respectively), in relationship to the Pro11→Leu polymorphism encoded by the minor allele (in brackets). The amino acids conserved in all species so far studied (i.e., human, marmoset, rabbit, and rat) (see Purdue et al. 1992*b*) are underlined. The double underline indicates the highly-conserved internal run of 58 amino acids (residues 133–190) referred to in the text. For this sequence the single letter amino acid code is used.

presumed to be metabolically inefficient in its role of glyoxylate detoxification when located in this organelle. Patients 1, 2, and 3 are unusual in that intermediate levels of AGT (52%–72%) are estimated to be located in the mitochondria.

Mutational analysis has clearly shown that all three patients are compound heterozygotes. All patients possess a novel mutation (G243→A) which is predicted to cause a Gly41→Arg amino acid substitution. In addition, two of the patients (1 and 2) possess an additional novel mutation (T576→A), which is predicted to cause a Phe152→Iso amino acid substitution. Patient 3 does not have the latter mutation, but instead has a previously recognized mutation (G630→A) which specifies a Gly170→Arg amino acid substitution (for a summary of the mutations and their allelic segregation, see table 4). The problem is to determine which mutation is responsible for which enzymological characteristic. Unfortunately, the three-dimensional structure of AGT has not been determined. Therefore the effects of any of these amino acid substitutions cannot yet be understood in structural terms. Nevertheless, computer predictions, based on the algorithms of Chou and Fasman (1974) and Garnier et al. (1978), indicate that at least some of these mutations could cause considerable local structural perturbations. Both algorithms predict that the Gly41→Arg replacement would lead to the generation of a stretch of α-helix from residues 36/37–41/46. On the other hand, the Phe152→Iso replacement is predicted to have either no effect (Chou and Fasman 1974) or only a small effect due to the extension of a small region of β-sheet by one residue (from 149–153 to 149–154) (Garnier et al. 1978).

All of the amino acid substitutions found in these patients occur in positions of high evolutionary conservation (fig. 8) (Oda et al. 1987; Takada et al. 1990; Purdue et al. 1992*b*). The amino acid substitutions Phe152→Iso and Gly170→Arg are situated close together on the same highly conserved internal region of 58 amino acids (Purdue et al. 1992*b*). Previous work on the study of the relationship between genotype and phenotype in the majority of PH1 patients with the peroxisome-to-mitochondrion trafficking defect has shown that the Gly170→Arg mutation and the Pro11→Leu polymorphism are both necessary for the full manifestation of the mistargeting phenomenon (Purdue et al. 1990). Pro11→Leu is predicted to lead to major structural alterations at the N-terminus of AGT which generate an amphiphilic α-helix characteristic of a mitochondrial targeting sequence (von Heijne 1986). Gly170→Arg has been predicted to inhibit the peroxisomal targeting/import of AGT by an as yet undetermined mechanism (Purdue et al. 1990). A control individual homozygous for the minor AGT allele (i.e., homozygous for the Pro11→Leu polymorphism) was shown to have only a small amount (5%) of AGT routed to the mitochondria (Purdue et al. 1990).

In patients 1 and 2, it would seem likely that Phe152→Iso fulfills a role similar to that of Gly170→Arg (i.e., it is responsible, together with the Pro11→Leu polymorphism, for the presence of mitochondrial AGT), while Gly170→Arg is responsible for this characteristic in patient 3. This role advocated for Phe152→Iso is compatible with the finding that two other PH1 patients (4 and 5) with low levels of mitochondrial AGT, but without peroxisomal cores, also possessed Phe152→Iso, albeit heterozygously, but not Gly41→Arg nor Gly170→Arg. In addition, the parents 1b and 2a, who carried Phe152→Iso (but not Gly41→Arg), showed the presence of mitochondrial AGT (estimated to be 13%–36% of total) in addition to

23%–46% of the normal level of soluble peroxisomal AGT (see table 2), again with no peroxisomal cores being found. The low level of mitochondrial AGT (~7%) in parent 1a, despite the absence of both Phe152→Iso and Gly170→Arg, is probably due to the homozygous presence of the Pro11→Leu polymorphism (see Purdue et al. 1990).

By default, Gly41→Arg, which is present in all three patients, is predicted to be concerned with the intraperoxisomal aggregation of AGT by a mechanism at present unknown. Parent 1a, who carried this mutation, possessed a small proportion of peroxisomes (~6%) containing core-like structures. When present, these were immunoreactive for AGT, but it was not possible to determine the specificity of labeling because of the presence of about half-normal levels of soluble AGT in the peroxisomal matrix, as expected for an obligate heterozygote. AGT is a homodimer (Takada and Noguchi 1982), and the small proportion of peroxisomes containing such AGT aggregations in a heterozygote might be due to the normal-mutant heterodimers remaining soluble and only the mutant homodimers being insoluble. This might be compounded by different efficiencies of peroxisomal import for the normal and mutant protein. This would not apply to the patients, because the polypeptide not possessing Gly41→Arg would not be imported into the peroxisomes but instead would be targeted to the mitochondria. Although only a minority of peroxisomal profiles appeared to possess cores, even in patients 1, 2, and 3, the relative sizes of the cores and peroxisomes (see table 2) would suggest that most of the 60-nm electron microscopic sections that cut through peroxisomes would "miss" the cores. An estimate can be made of the likely real percentage of peroxisomes containing cores, which works out to be about 57%–82% for patients 1, 2, and 3, and about 16% for parent 1a.

Additional studies provide circumstantial evidence against the polypeptide containing the Gly41→Arg substitution being present to any significant extent in the mitochondria in vivo in patients 1, 2, and 3, despite the presence of a mitochondrial targeting sequence (because of the presence of the Pro11→Leu polymorphism). Unlike most "normal" mitochondrial targeting sequences, including those found in marmoset and rat premitochondrial AGT (Oda et al. 1987; Purdue et al. 1992*b*), the "abnormal" one found in AGT possessing the Pro11→Leu polymorphism is not cleaved on import by mitochondria in vitro, presumably because of a lack of an appropriate cleavage recognition site (Purdue et al. 1991*a*). The nascent in vitro transcribed/translated AGT polypeptide containing the Pro11→Leu plus Gly41→Arg amino acid substitutions is imported into mitochondria in vitro, as expected, because of the presence of the mitochondrial targeting sequence (data not shown) (see Purdue et al. 1991*a*). However, preliminary evidence suggests that cleavage of this mutant polypeptide *does* occur after in vitro mitochondrial import to produce a polypeptide about 4 kDa smaller (i.e., about 39 kDa instead of the normal size of 43 kDa). The reason for this is unknown but might be related to the introduction of a recognized cleavage site, due to the Gly→Arg replacement at amino acid position 41. Most mitochondrial precursor proteins, including the marmoset and rat AGT mitochondrial precursor (Oda et al. 1987; Purdue et al. 1992*b*), possess Arg at position −2 relative to the site of cleavage (Hendrick et al. 1989). However, a polypeptide of this size (i.e., 39 kDa) is not found in patients 1, 2, or 3 when analyzed by SDS-PAGE, indicating that the Pro11→Leu plus Gly41→Arg mutant polypeptide is either not significantly imported into mitochondria in vivo or that, if it is, it is rapidly degraded.

The relationship between the various mutations found in these patients and the low level of AGT immunoreactivity and complete, or nearly complete, absence of AGT catalytic activity is not understood. PH1 patients who are heterozygous for the Pro11→Leu plus Gly170→Arg substitutions and who also fail to express the apparently "normal" allele have been shown to have much reduced AGT levels that varied from 0%–13% (Purdue et al. 1990). It might be that the mutations described in this paper have additional effects on the AGT structure, which influence protein stability and import efficiency, so that much of the nascent protein is prematurely degraded. There is no evidence for reduced levels of transcription or reduced mRNA stability. Northern blotting demonstrated the presence of normal levels of AGT mRNA in the liver of patient 1 (data not shown). Further studies will be required to distinguish between these possibilities and to determine the exact molecular mechanism behind the remarkable finding of intraperoxisomal AGT aggregation.

## Acknowledgments

The anti-rat peroxisomal thiolase, peroxisomal hydratase, and acyl-CoA oxidase antibodies were a gift from Professor A. Völkl (University of Heidelberg), the anti-rat glycolate oxidase antibody from Professor T. Hashimoto (Shinshu University School of Medicine), and the anti-rat urate oxidase antibody from Dr. S. Yokota (Yamanashi Medical College). The clinical studies on family 1 were carried out at the Clinical Research Center of the University of Chicago, with support

from USPHS grant MO1 RR 00055 and the Liver Research Fund of the University of Chicago, on family 2 at the Variety Club Children's Hospital, University of Minnesota, and on family 3 at the Duke University Medical Center.

## References

Afzelius BA (1965) The occurrence and structure of microbodies: a comparative study. J Cell Biol 26:835–843

Allsop J, Jennings PR, Danpure CJ (1987) A new micro-assay for human liver alanine:glyoxylate aminotransferase. Clin Chim Acta 170:187–193

Angermuller S, Fahimi HD (1986) Ultrastructural cytochemical localization of uricase in peroxisomes of rat liver. J Histochem Cytochem 34:159–165

Biempica L (1966) Human hepatic microbodies with crystalloid cores. J Cell Biol 29:383–386

Carlemalm E, Garavito RM, Villiger W (1982) Resin development for electron microscopy and an analysis of embedding at low temperature. J Microsc 126:123–143

Chomczynski P, Sacchi N (1987) Single-step method of RNA isolation by acid guanidinium thiocyanate-phenol-chloroform extraction. Anal Biochem 162:156–159

Chou PY, Fasman GD (1974) Prediction of protein structure. Biochemistry 13:222–245

Collins JC, Scheinberg IH, Giblin DR, Sternlieb I (1989) Hepatic peroxisomal abnormalities in abetalipoproteinemia. Gastroenterology 97:766–770

Cooper PJ, Danpure CJ, Wise PJ, Guttridge KM (1988*a*) Immunocytochemical localization of human hepatic alanine: glyoxylate aminotransferase in control subjects and patients with primary hyperoxaluria type 1. J Histochem Cytochem 36:1285–1294

——— (1988*b*) Immunoelectron-microscopic localisation of alanine:glyoxylate aminotransferase in normal human liver and type 1 hyperoxaluric livers. Biochem Soc Trans 16: 627–628

Danpure CJ (1991) Molecular and clinical heterogeneity in primary hyperoxaluria type 1. Am J Kidney Dis 17:366–369

Danpure CJ, Cooper PJ, Wise PJ, Jennings PR (1989) An enzyme trafficking defect in two patients with primary hyperoxaluria type 1: peroxisomal alanine/glyoxylate aminotransferase rerouted to mitochondria. J Cell Biol 108: 1345–1352

Danpure CJ, Guttridge KM, Fryer P, Jennings PR, Allsop J, Purdue PE (1990) Subcellular distribution of hepatic alanine:glyoxylate aminotransferase in various mammalian species. J Cell Sci 97:669–678

Danpure CJ, Jennings PR (1986) Peroxisomal alanine:glyoxylate aminotransferase deficiency in primary hyperoxaluria type I. FEBS Lett 201:20–24

——— (1988) Further studies on the activity and subcellular distribution of alanine:glyoxylate aminotransferase in the livers of patients with primary hyperoxaluria type 1. Clin Sci 75:315–322

De Netto LA, Tappia PS, Malik ZA, Wood AJ, Mann VM, Jones CJ, Burdett K, et al (1991) Human hepatic peroxisomes with crystalloid cores associated with urate oxidase activity. Adv Exp Med Biol 309A:373–376

Garnier J, Ogusthorpe DJ, Robson B (1978) Analysis of the accuracy and implications of simple methods for predicting the secondary structure of globular proteins. J Mol Biol 120:97–120

Grzybek H, Panz B, Petelenz M, Gonciarz Z, Kusmierski S, Kocek B (1986) Three cases of human peroxisomes with crystalloid core. Eur J Cell Biol 41:16

Hendrick JP, Hodges PE, Rosenberg LE (1989) Survey of amino-terminal proteolytic cleavage sites in mitochondrial precursor proteins: leader peptides cleaved by two matrix proteases share a three-amino acid motif. Proc Natl Acad Sci USA 86:4056–4060

Jansen R, Ledley FD (1990) Disruption of phase during PCR amplification and cloning of heterozygous target sequences. Nucleic Acids Res 18:5153–5156

Laemmli UK (1970) Cleavage of structural proteins during the assembly of the head of bacteriophage T4. Nature 227:680–685

Lowry OH, Rosebrough NJ, Farr AL, Randall RJ (1951) Protein measurement with the folin-phenol reagent. J Biol Chem 193:265–275

Minatogawa Y, Tone S, Allsop J, Purdue PE, Takada Y, Danpure CJ, Kido R (1992) A serine-to-phenylalanine substitution leads to loss of alanine:glyoxylate aminotransferase catalytic activity and immunoreactivity in a patient with primary hyperoxaluria type 1. Hum Mol Genet 1:643–644

Nishiyama K, Funai T, Katafuchi R, Hattori F, Onoyama K, Ichiyama A (1991) Primary hyperoxaluria type I due to a point mutation of T to C in the coding region of the serine:pyruvate aminotransferase gene. Biochem Biophys Res Commun 176:1093–1099

Noguchi T, Takada Y (1978) Peroxisomal localization of serine:pyruvate aminotransferase in human liver. J Biol Chem 253:7598–7600

——— (1979) Peroxisomal localization of alanine: glyoxylate aminotransferase in human liver. Arch Biochem Biophys 196:645–647

Oda T, Miyajima H, Suzuki Y, Ichiyama A (1987) Nucleotide sequence of the cDNA encoding the precursor for mitochondrial serine:pyruvate aminotransferase of rat liver. Eur J Biochem 168:537–542

Purdue PE, Allsop J, Isaya G, Rosenberg LE, Danpure CJ (1991*a*) Mistargeting of peroxisomal L-alanine:glyoxylate aminotransferase to mitochondria in primary hyperoxaluria patients depends upon activation of a cryptic mitochondrial targeting sequence by a point mutation. Proc Natl Acad Sci USA 88:10900–10904

Purdue PE, Lumb MJ, Allsop J, Danpure CJ (1991*b*) An intronic duplication in the alanine:glyoxylate aminotransferase gene facilitates identification of mutations in compound heterozygote patients with primary hyperoxaluria type 1. Hum Genet 87:394–396

Purdue PE, Lumb MJ, Allsop J, Minatogawa Y, Danpure CJ

(1992*a*) A glycine-to-glutamate substitution abolishes alanine:glyoxylate aminotransferase catalytic activity in a subset of patients with primary hyperoxaluria type 1. Genomics 13:215–218

Purdue PE, Lumb MJ, Danpure CJ (1992*b*) Molecular evolution of alanine:glyoxylate aminotransferase 1 intracellular targeting: analysis of the marmoset and rabbit genes. Eur J Biochem 207:757–766

Purdue PE, Lumb MJ, Fox M, Griffo G, Hamon Benais C, Povey S, Danpure CJ (1991*c*) Characterization and chromosomal mapping of a genomic clone encoding human alanine:glyoxylate aminotransferase. Genomics 10:34–42

Purdue PE, Takada Y, Danpure CJ (1990) Identification of mutations associated with peroxisome-to-mitochondrion mistargeting of alanine/glyoxylate aminotransferase in primary hyperoxaluria type 1. J Cell Biol 111:2341–2351

Roth J (1982) The protein A-gold (pAg) technique: a quantitative and qualitative approach for antigen localization on thin sections. In: Bullock GR, Petrusz P (eds) Techniques in immunocytochemistry. Academic Press, London, pp 108–133

Sambrook J, Fritsch EF, Maniatis T (1989) Molecular cloning: a laboratory manual. Cold Spring Harbor Laboratory, Cold Spring Harbor, New York

Sternlieb I, Quintana N (1977) The peroxisomes of human hepatocytes. Lab Invest 36:140–149

Takada Y, Kaneko N, Esumi H, Purdue PE, Danpure CJ (1990) Human peroxisomal L-alanine: glyoxylate aminotransferase: evolutionary loss of a mitochondrial targeting signal by point mutation of the initiation codon. Biochem J 268:517–520

Takada Y, Noguchi T (1982) Subcellular distribution, and physical and immunological properties of hepatic alanine: glyoxylate aminotransferase isoenzymes in different mammalian species. Comp Biochem Physiol (B) 72:597–604

Teng B-B, Verp M, Salomon J, Davidson NO (1990) Human apolipoprotein B messenger RNA editing is developmentally modulated and expressed in tissues other than small intestine. J Biol Chem 265:20616–20620

Thompson JS, Richardson KE (1967) Isolation and characterization of an L-alanine:glyoxylate aminotransferase from human liver. J Biol Chem 242:3614–3619

Towbin H, Staehelin T, Gordon J (1979) Electrophoretic transfer of proteins from polyacrylamide gels to nitrocellulose sheets: procedure and some applications. Proc Natl Acad Sci USA 76:4350–4354

Varela Echavarria A, Montes de Oca Luna R, Barrera Saldana HA (1988) Uricase protein sequences: conserved during vertebrate evolution but absent in humans. FASEB J 2:3092–3096

Völkl A, Baumgart E, Fahimi HD (1988) Localization of urate oxidase in the crystalline cores of rat liver peroxisomes by immunocytochemistry and immunoblotting. J Histochem Cytochem 36:329–336

von Heijne G (1986) Mitochondrial targeting sequences may form amphiphilic helices. EMBO J 5:1335–1342

Watts RWE, Danpure CJ, de Pauw L, Toussaint C (1991) Combined liver-kidney and isolated liver transplantations for primary hyperoxaluria type 1: the European experience. Nephrol Dial Transpl 6:502–511

Williams HE, Smith LH (1983) Primary hyperoxaluria. In: Stanbury JB, Wyngaarden JB, Fredrickson DS, Goldstein JL, Brown MS (eds) The metabolic basis of inherited disease. McGraw-Hill, New York, pp 204–228

Wise PJ, Danpure CJ, Jennings PR (1987) Immunological heterogeneity of hepatic alanine:glyoxylate aminotransferase in primary hyperoxaluria type 1. FEBS Lett 222:17–20

Wu XW, Lee CC, Muzny DM, Caskey CT (1989) Urate oxidase: primary structure and evolutionary implications. Proc Natl Acad Sci USA 86:9412–9416

Yeldandi AV, Wang X, Alvares K, Kumar S, Rao MS, Reddy JK (1990) Human urate oxidase gene: cloning and partial sequence analysis reveal a stop codon within the fifth exon. Biochem Biophys Res Commun 171:641–646

Yokota S, Oda T, Ichiyama A (1987) Immunocytochemical localization of serine:pyruvate aminotransferase in peroxisomes of the human liver parenchymal cells. Histochemistry 87:601–606